Rechargeable organic lithium-ion batteries using electron-deficient benzoquinones as positive-electrode materials with high discharge voltages

ARTICLE

Rechargeable organic lithium-ion batteries using electron-deficient benzoquinones as positive-electrode materials with high discharge voltages†

Takato Yokoji,[a] Hiroshi Matsubara*[a] and Masaharu Satoh[b]

Organic rechargeable lithium-ion batteries have great potential to overcome the various problems of current inorganic battery configurations. Although organic quinone-type positive-electrode materials have been previously applied in batteries, their inferior voltage output compared to those using $LiCoO_2$ signifies the need for further development. Thus, we focused on raising the voltages from benzoquinone derivatives through use of structural diversity. Electron-deficient benzoquinones bearing perfluoroalkyl groups were prepared and evaluated as cathode active materials in rechargeable batteries. The cells exhibited higher voltage plateaus in their charge-discharge curves compared to those using electron-rich benzoquinones, indicating the increased voltage as a result of the electron-withdrawing groups in the benzoquinone skeleton. The perfluoroalkylated benzoquinones effectively worked as positive-electrode materials, with improved charge-discharge cycle performance in the cells due to the stability of the benzoquinones toward decomposition during cycling. DFT calculations performed to explore the reasons behind this stability revealed that Li-F interactions stabilized the radical and dilithium-salt intermediates of benzoquinone reduction. Electrolyte effects on the charge-discharge performance were also examined in the trifluoromethylated system, revealing a significant impact on the shape of the discharge curves and the cycle-life performance.

Introduction

In this age of high energy consumption, rechargeable batteries are indispensable for the storage of electrical energy.[1] Lithium-ion batteries (LIBs) that employ $LiCoO_2$ as the cathode active material (with a capacity of 150–170 Ah/kg and a voltage of 3.7 V versus Li/Li^+) have emerged as high-performance rechargeable battery systems, and are the primary energy sources used in mobile phones and laptop computers.[2] However, LIBs can be problematic in terms of safety and material resource availability (cobalt). For example, the batteries are known to be at risk of explosion when short-circuited or overcharged. In addition, the electrical capacity development in LIBs will have difficulty maintaining pace with the increasing energy demands of electrical devices.[3]
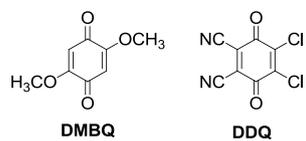
Rechargeable batteries using organic cathode active materials can solve these problems. The large structural diversity of organic compounds allows the preparation of myriad cells which may provide higher mass energy densities than those using inorganic compounds. In addition, many organic compounds undergo reversible redox reactions with two or more electrons, which would endow the battery with high capacity. Indeed, organic cathode materials are expected to function as substitutes for $LiCoO_2$, and significant numbers of organic compounds have been evaluated.[4] The previously reported materials can generally be categorized into three types. The first are organosulfur compounds,[5] as exemplified by disulfides and thioethers. These compounds commonly exhibit high capacities but low voltages.[6] The second type consists of the radical compounds, such as nitroxides, which generally have low capacities.[4,7] However, the discharge voltages of these compounds are relatively high among the organic positive-electrode materials. The third type are carbonyl compounds,[4,8] of which benzoquinone (BQ) derivatives, which show reversible two-electron redox behavior, are representative examples. Most carbonyl compounds afford high capacities but low voltages. In recent years, other types of organic positive-electrode materials have been investigated.[4,8c,9]

The cycle-life performance of low-molecular-weight organic electrode-active materials is generally poor because of the dissolution of the small molecules into the electrolyte.[4,10] Therefore, organic polymers have been examined as cathode active materials for rechargeable batteries. Although

polymerization prevents the materials from dissolving, it also tends to reduce the capacity to much lower levels than the theoretical capacity of the monomer unit.[4,11] Recently, quasi-solid state or two-compartment lithium batteries using low-molecular-weight organic compounds as positive-electrode materials were reported.[12,13] In these reports, the applied materials gave high cycle-life performance without the use of polymers of the small organic compounds as cathodes, suggesting their potential utility with further study.

BQs are expected to afford high capacities since they have a simple, low-molecular-weight skeleton and can function as two-electron acceptors. Batteries using BQ derivatives showed high capacities, but their discharge voltages were low.[10b,12b,13,14] For example, 2,5-dimethoxy-1,4-benzoquinone (DMBQ) was utilized as a positive-electrode material in a rechargeable LIB.[14b,14c] In this case, the average discharge voltage was only 2.6 V versus Li/Li$^+$. On the other hand, a battery using 2,3-dichloro-5,6-dicyano-1,4-benzoquinone (DDQ)[14a] showed high voltage plateaus of 3.4 and 3.2 V, but it gave a low capacity of about 55 Ah/kg in the first cycle,[12b] which did not reach half of the capacity of a battery using LiCoO$_2$. Thus, it has been difficult to establish a high energy density with a high voltage in BQ derivatives.

In order to exceed the performance of the current LIBs, the combination of high discharge voltage with high capacity is desired in batteries using organic materials. The capacity of a battery C_{theo} (Ah/kg) is defined based on the molecular weight M and number of electrons participating in the redox reaction Z in a positive-electrode material:

$$C_{theo} = 26800 \cdot Z/M \qquad (1)$$

However, the relationship between the molecular structures of organic positive-electrode materials and discharge voltages is not well understood.

We recently synthesized electron-deficient BQs bearing perfluoroalkyl groups, which are well known as strong electron-withdrawing substituents, and used them as oxidizing agents (Fig. 1).[15] The prepared BQs revealed two reversible redox steps. In the cyclic voltammograms (CVs) of acetonitrile solutions of 2,5-dimethyl-1,4-benzoquinone (CH$_3$-BQ), 2,5-bis(trifluoromethyl)-1,4-benzoquinone (CF$_3$-BQ), 2,5-bis(perfluorobutyl)-1,4-benzoquinone (Rf$_4$-BQ), and 2,5-bis(perfluorohexyl)-3,6-dichloro-1,4-benzoquinone (Rf$_6$-Cl-BQ), the first reduction peak potentials (E$_{1p,c}$) were −1.08, −0.41, −0.38 and −0.26 V vs. Ag/Ag$^+$, respectively (Fig. 2), indicating that BQs bearing perfluoroalkyl groups functioned as strong electron acceptors. These results prompted us to prepare rechargeable batteries using the perfluoroalkylated BQs as positive-electrode materials, to overcome the deficiencies of BQs in such roles and afford both high discharge voltages and high capacities. Herein, we report the preparation and electrochemical properties of rechargeable batteries using CH$_3$-

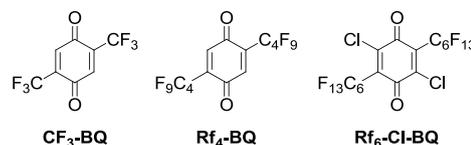BQ, CF$_3$-BQ, Rf$_4$-BQ, and Rf$_6$-Cl-BQ as positive-electrode materials.

Fig. 1 Electron-deficient benzoquinones bearing perfluoroalkyl groups.
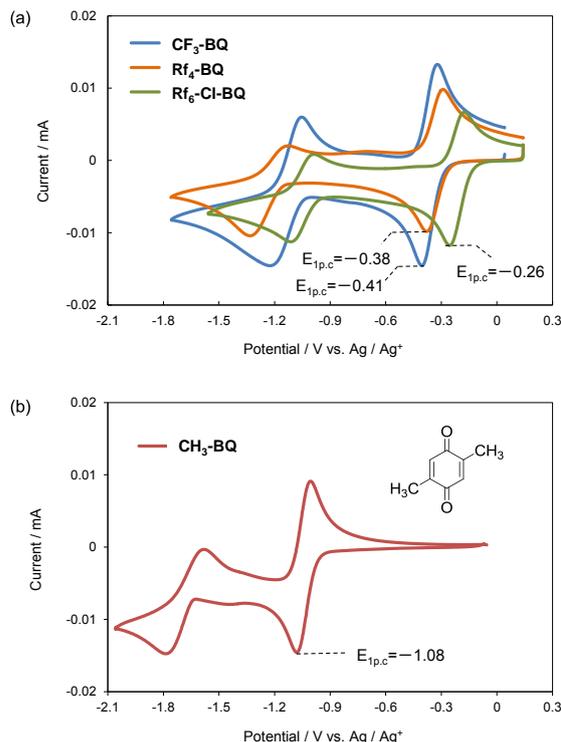

Fig. 2 Solution CVs of (a) electron-deficient benzoquinones bearing perfluoroalkyl groups (CF$_3$-BQ, Rf$_4$-BQ and Rf$_6$-Cl-BQ) and (b) an electron-rich benzoquinone (CH$_3$-BQ).

Results and discussion

Charge–discharge curves and cycle performance of BQ-based rechargeable batteries

We prepared CF$_3$-BQ, Rf$_4$-BQ, and Rf$_6$-Cl-BQ as described in our recent paper.[15] CH$_3$-BQ was purchased and used without further purification. The battery performance of the BQs was examined by preparing coin-type cells containing 3 wt% of the positive-electrode materials (BQs). The electrolyte solution was a mixture of ethylene carbonate (EC, 30 vol%) and diethyl carbonate (DEC, 70 vol%) containing 1.0 M LiPF$_6$. Fig. 3 shows the charge-discharge curves and cycle-life performance over eighth cycles for cells with the four positive-electrode materials. The first discharge capacity of the cell using CF$_3$-BQ was 162 Ah/kg, which was lower than that of CH$_3$-BQ (320 Ah/kg), because of the higher molecular weight of CF$_3$ versus CH$_3$. The first discharge process of the cell using CF$_3$-BQ

showed two voltage plateaus at 3.0 and 2.9 V (average voltage: 3.0 V versus Li/Li$^+$), which were higher than that of CH$_3$-BQ (a plateau at 2.7 V). Moreover, the charge-discharge behavior of the cell using CF$_3$-BQ was more stable than that of CH$_3$-BQ. The shapes of the charge-discharge curves for the CF$_3$-BQ cell were hardly changed with cycle number, while the shapes of the curves for the CH$_3$-BQ cell were significantly changed from the first cycle to the second, and the second cycle to the third. This charge-discharge behavior of the CF$_3$-BQ cell was also observed in the Rf$_4$-BQ cell (first discharge capacity: 115 Ah/kg, voltage plateau of first discharge process: 3.0 V). Surprisingly, the first discharge capacity of the Rf$_6$-Cl-BQ cell (177 Ah/kg) exceeded the theoretical value of 66 Ah/kg (2 electrons). This observation was rationalized by considering that Rf$_6$-Cl-BQ acted as more than a two-electron acceptor.

The cycle-life performance for the cells evaluated over 20 cycles is shown in Fig. 4, and the electrochemical parameters of the BQs are summarized in Table 1. The cycle-life performance of the CH$_3$-BQ-based cell was obviously worse than those of the perfluoroalkylated BQs. This was reflected by the significant changes in the charge-discharge curve shapes for the CH$_3$-BQ-based cell, which indicated the remarkable decrease in capacity. The cycle-life performance of the cell using Rf$_6$-Cl-BQ was better than those of the CF$_3$- and Rf$_4$-BQ cells. The ratio of the 20th discharge capacity to the first was 55% (capacity of 20th cycle: 98 Ah/kg) in Rf$_6$-Cl-BQ, 50% (capacity of 20th cycle: 58 Ah/kg) in Rf$_4$-BQ, and 37% (capacity of 20th cycle: 60 Ah/kg) in CF$_3$-BQ. It is well known that the introduction of perfluoroalkyl groups into organic molecules imparts lipophobicity, which would suppress the dissolution of materials in the electrolyte and improve cycle-life performance. The order of E$_{1p,c}$ values (CH$_3$-BQ < CF$_3$-BQ < Rf$_4$-BQ < Rf$_6$-Cl-BQ) in the solution CVs corresponds to that of the average discharge voltages, which indicates that the more electron-deficient BQs (i.e., those with many strong electron-withdrawing groups) would afford higher discharge voltages when used as positive-electrode materials. In a previous report on organic cathode-active materials, molecules with larger energy gaps between the LUMO and HOMO levels afforded higher discharge voltages.[10e] On this basis, we examined the energy gaps via theoretical quantum calculations using density functional theory (DFT). The order of the calculated energy gaps of the BQs was found to correspond to the order of the E$_{1p,c}$ values in the solution CVs (Supplementary Information, Table S1). Thus, introducing electron-withdrawing groups in the BQ skeleton reduced the LUMO/HOMO energy gaps, lowered the E$_{1p,c}$ values in the solution CVs, and increased the discharge voltages in the batteries.
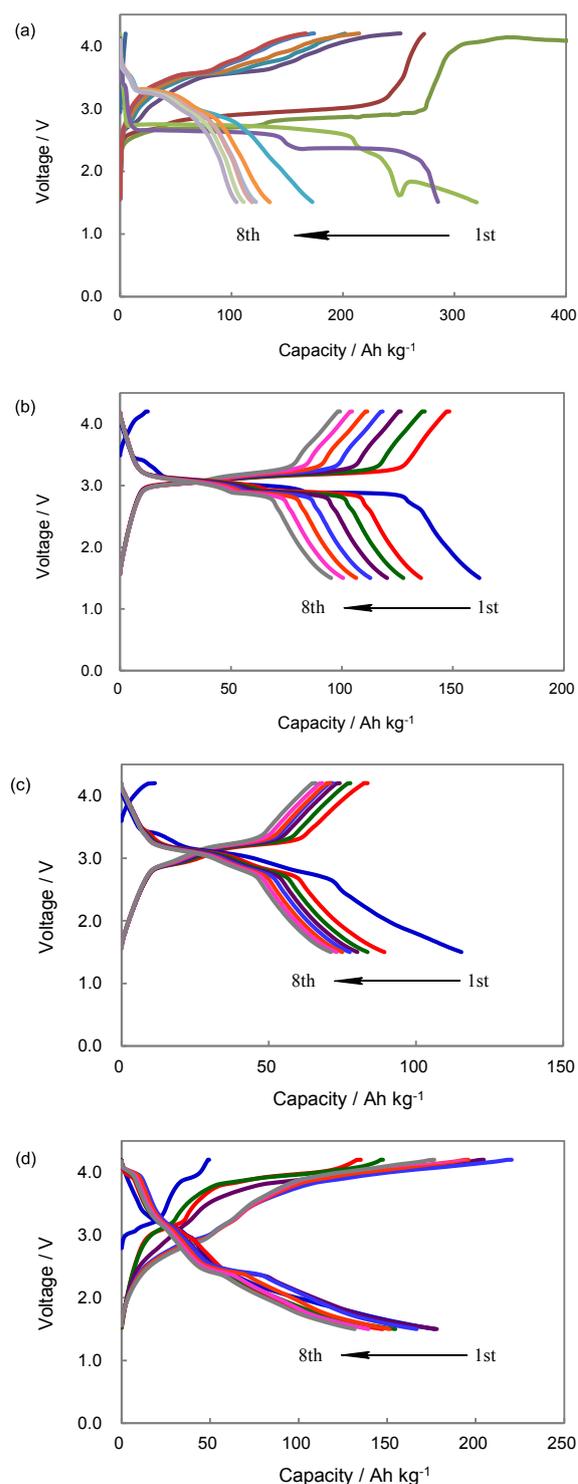

Fig. 3 Charge-discharge curves and cycle-life performance over eight cycles for (a) CH$_3$-BQ, (b) CF$_3$-BQ, (c) Rf$_4$-BQ and (d) Rf$_6$-Cl-BQ.

Table 1 Electrochemical parameters of benzoquinones bearing methyl or perfluoroalkyl groups.

Sample	$E_{1p, c}$ in solution CV (V)	Average discharge voltage (V)		Theoretical capacity (Ah/kg)	Practical capacity (Ah/kg)		
		1st cycle	2nd		1st cycle	2nd	20th
CH_3-BQ	-1.08	2.7	2.5	394	320	285	68 (21%)[a]
CF_3-BQ	-0.41	3.0	3.0	220	162	136	60 (37)
Rf_4-BQ	-0.38	3.0	3.1	99	115	89	58 (50)
Rf_6-Cl-BQ	-0.26	3.1	3.1	66	177	147	98 (55)

[a] Ratio of the capacity to the 1st cycle.
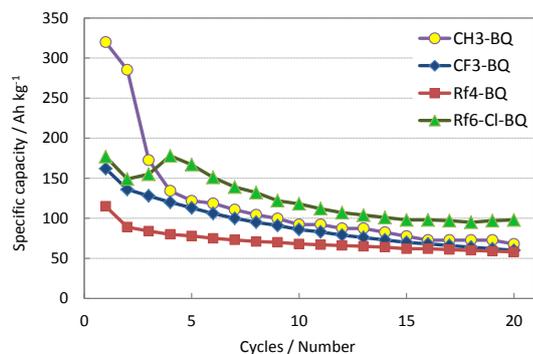
Fig. 4 Cycle-life performance over twentieth cycles for cells based on CH_3-BQ, CF_3-BQ, Rf_4-BQ, and Rf_6-Cl-BQ.

Cyclic voltammetry of electrodes using BQs

The CVs of the electrodes in the prepared cells are shown in Fig. 5. The shape of the voltammogram for the CH_3-BQ cell at the first cycle was slightly different from those after the second and third cycles. This trend was also observed in the charge-discharge curves for CH_3-BQ (Fig. 3a), which indicated its possible decomposition during cycling. It may be that the methyl group in CH_3-BQ is unstable toward charge-discharge cycling because of its reactive allylic hydrogens. Except for the shape change over three cycles, the redox behaviors of CH_3-BQ and CF_3-BQ are similar, affording reversible two-electron redox reactions from the first cycle to the eighth. Although Rf_4-BQ gave a reversible two-electron redox step similar to those of CH_3-BQ and CF_3-BQ, an extra reduction peak of high intensity was observed at 3.5 V in only the first cycle. This extra reduction peak indicates that further redox reaction occurs. Consequently, the observed discharge capacity for the first cycle in the Rf_4-BQ cell (115 Ah/kg) exceeds the theoretical value (99 Ah/kg). A similar extra reduction peak can be found at 3.5 V in the first cycle in the CF_3-BQ cell. However, the intensity of that extra peak is much lower than the other peaks. Therefore, unlike the Rf_4-BQ cell, the observed capacity for the CF_3-BQ cell (162 Ah/kg) does not exceed the theoretical value (220 Ah/kg). The shapes of the voltammograms of Rf_6-Cl-BQ change with increasing cycle number, especially between the first and the third, indicating that irreversible reactions occur in the electrode. This is supported by the slight variation in shape between the first and the second discharge curves for the cell (Fig. 3d). Longer perfluoroalkylated BQs showed more complex electrode CV behavior than can be predicted from the

general redox chemistry of benzoquinones, and their observed capacities exceeded theoretical predictions. Accordingly, introducing longer perfluoroalkyl groups into the BQ skeleton might allow the acceptance of two or more electrons in the molecule. However, the detailed redox mechanism of perfluoroalkylated BQs in the cell is not clear at present, and is under investigation.
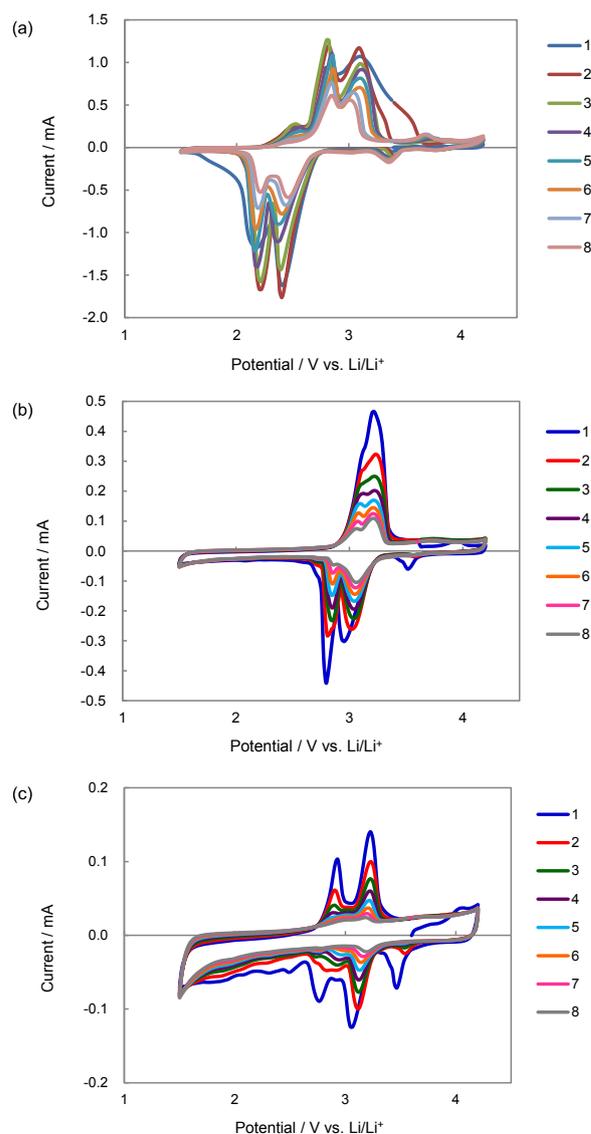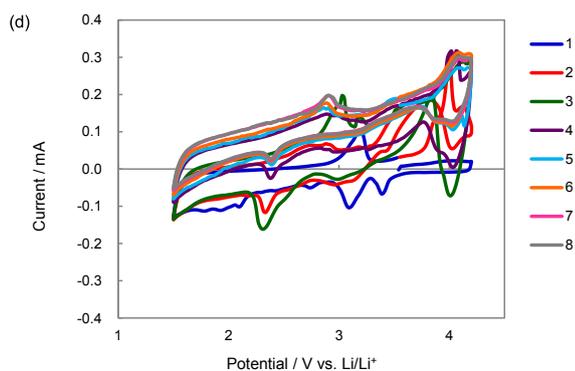
Fig. 5 Cyclic voltammograms of electrodes containing (a) CH₃-BQ, (b) CF₃-BQ, (c) Rf₄-BQ, and (d) Rf₆-Cl-BQ in 1.0 M LiPF₆-EC/DEC. Cycle numbers are indicated by the line colors in the legends

DFT study on radical and dilithium-salt states of BQs

As mentioned above, the shapes of the charge-discharge curves of BQs bearing perfluoroalkyl groups hardly changed with increasing cycle number, whereas that of CH₃-BQ was significantly changed from the first cycle to the second, and the second to the third, indicating its considerable decrease in capacity. The proposed charge-discharge mechanism for the BQ derivatives in the cells is shown in Scheme 1.
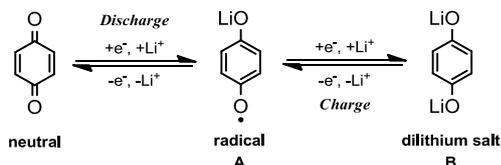
Scheme 1 Proposed charge-discharge mechanism for benzoquinone as a positive-electrode material in a rechargeable LIB.

Neutral BQ accepts an electron and Li⁺ to afford the radical species **A**. Radical **A** accepts another electron and Li⁺ to generate dilithium salt **B**. The mechanism for the charge process is the reverse of the discharge one. In the event radical **A** or dilithium salt **B** is unstable, side reactions may occur, which would change the shape of the charge-discharge curves with increasing numbers of cycles. To ascertain the structural features and stability of the radical and dilithium-salt species, we performed DFT calculations. The optimized structures of the radicals and dilithium salts of CH₃-BQ and CF₃-BQ are shown in Fig. 6. The calculated bond angles for C–O–Li in the radical and dilithium salt of CH₃-BQ are almost 180°, while those in CF₃-BQ are 123–124°. Bond distances for Li-F in the radical and dilithium salt of CF₃-BQ were predicted to be around 2.12 Å, indicating that a significant interaction between lithium and the fluorine atoms exists in both species for CF₃-BQ. Similar Li-F interactions were observed in optimized structures involving Rf₄-BQ and Rf₆-Cl-BQ (Supplementary information, Fig. S1). The energy profiles of the BQs in the

neutral, radical, and dilithium-salt states are depicted in Fig. 7. As shown, the radicals of the BQs (+ Li) are more stable than the neutral BQs (+ 2Li), and the dilithium salts of the BQs are more stable than the radicals (+ Li). Importantly, the stabilization energies (ΔE₁ and ΔE₂) of CF₃-BQ are similar to those of Rf₄-BQ and Rf₆-Cl-BQ, and obviously lower than those of CH₃-BQ (Table 2). The Li-F interactions in the perfluoroalkylated BQs effectively stabilize the radical and the dilithium-salt states, which is important for obtaining good charge-discharge performance.
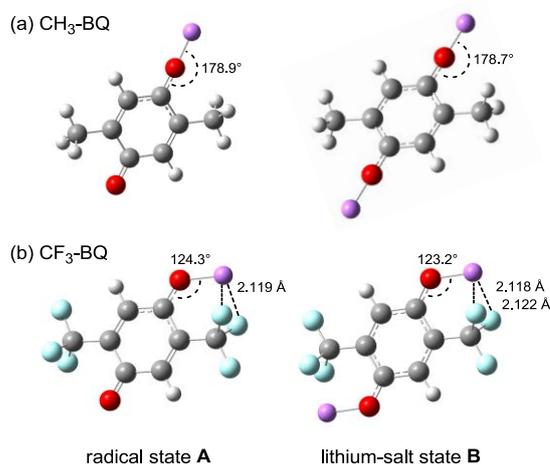

Fig. 6 Optimized structures of (a) CH₃-BQ and (b) CF₃-BQ in radical **A** and dilithium-salt **B** states by DFT calculations. Atom colors : C, gray; H, white; O, red; F, aqua; Li, purple.
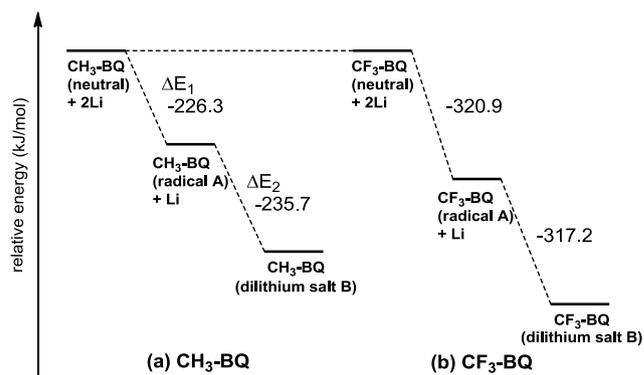

Fig. 7 Stabilization Energies, ΔE₁ (= ($E_{radical}$ + E_{Li}) − ($E_{neutral}$ + 2E_{Li})) and ΔE₂ (= $E_{dilithium\ salt}$ − ($E_{radical}$ + E_{Li})) of (a) CH₃-BQ and (b) CF₃-BQ by DFT calculations.

Table 2 Stabilization Energies, ΔE_1 and ΔE_2 of benzoquinones based on DFT calculations.

Sample	Stabilization Energy (kJ/mol)	
	ΔE_1	ΔE_2
CH_3-BQ	-226.3	-235.7
CF_3-BQ	-320.9	-317.2
Rf_4-BQ	-329.3	-324.1
Rf_6-Cl-BQ	-332.7	-334.3

$\Delta E_1 = (E_{radical} + E_{Li}) - (E_{neutral} + 2E_{Li})$, $\Delta E_2 = E_{dilithium\ salt} - (E_{radical} + E_{Li})$

Electrolyte effects in charge–discharge curves and cycle performance

Electrolyte effects in a coin-type cell of CF_3-BQ were examined to improve the cycle performance of the batteries. In these experiments, the coin-type cells contained 5 wt% positive-electrode material (CF_3-BQ), and either ethyl isopropyl sulfone (EiPS) containing 1.0 M $LiN(SO_2CF_3)_2$ (LiTFSI) or triethylene glycol dimethyl ether (tetraglyme) containing 4.8 M LiTFSI. The LiTFSI-tetraglyme system provided a first discharge capacity of 164 Ah/kg, and the average discharge voltage in the first cycle was 3.0 V (Fig. 8a); the discharge capacity and voltage were similar to those of $LiPF_6$-EC/DEC (Fig. 3b). On the other hand, the LiTFSI-EiPS system revealed a first discharge capacity of 209 Ah/kg (Fig. 8b), which was superior to that of the $LiPF_6$-EC/DEC system and close to the theoretical value, 220 Ah/kg. The first discharge process in this system showed two voltage plateaus at 3.1 and 2.9 V (average voltage: 3.0 V), similarly to the $LiPF_6$-EC/DEC system. The ratio of the twentieth discharge capacity to the first was 37% (capacity of twentieth cycle: 60 Ah/kg) in $LiPF_6$-EC/DEC, 29% (capacity of twentieth cycle: 48 Ah/kg) in LiTFSI-tetraglyme, and 23% (capacity of twentieth cycle: 48 Ah/kg) in LiTFSI-EiPS (For cycle-life performance data, see supplementary information, Fig. S2). These results indicate that using LiTFSI-EiPS as an electrolyte in a rechargeable battery employing CF_3-BQ gives the highest discharge capacity and the lowest cycle-life performance, whereas using $LiPF_6$-EC/DEC affords the lowest discharge capacity and the highest cycle-life performance.

Redox reactions involving two electrons for benzoquinones as a cathode active material in rechargeable LIBs would proceed stepwise; this can be observed as the two plateaus in the discharge curves for the CF_3-BQ cells in the $LiPF_6$-EC/DEC and LiTFSI-EiPS systems. On the other hand, in LiTFSI-tetraglyme system, the discharge plateau is difficult to distinguish, and the discharge curve decreases gradually. The stability of the radical state of a BQ would be the key to the appearance of the plateaus. Generally, the neutral state of a redox-active molecule accepts one electron to afford its radical state, which corresponds to the first plateau, and the resultant radical accepts another electron to generate a dilithium salt, which corresponds to the second plateau. When the two reactions proceed stepwise, two plateaus are observed.

However, if they proceed in parallel, the discharge curves would not afford two plateaus and would decrease gradually. Stable radical species afford stepwise redox reactions while unstable ones easily accept another electron before completion of the first reduction step. Therefore, electrolytes which would stabilize the BQ radical state might effectively stabilize the discharge voltages. Although detailed mechanisms have not been elucidated, research on electrolyte effects in BQ-based cells would be valuable in the exploration of battery performance trends with organic cathode active materials.
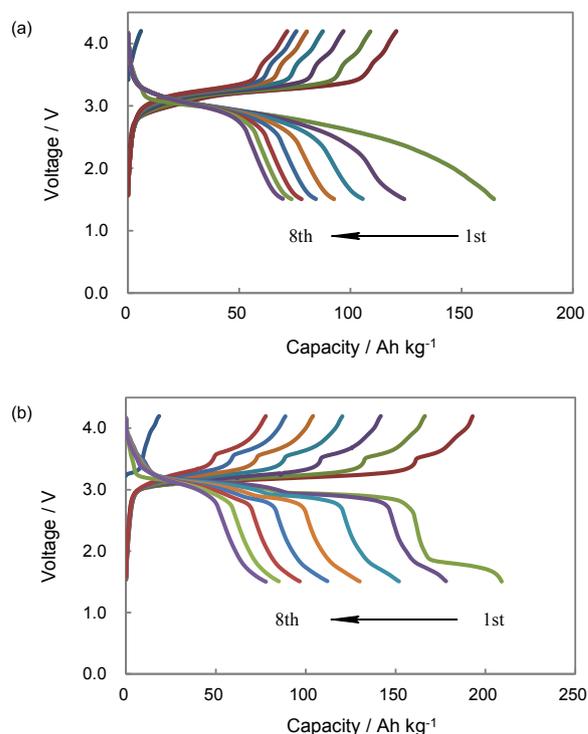

Fig. 8 Charge-discharge curves and cycle-life performance over eight cycles, using CF_3-BQ in (a) 4.8 M-LiTFSI in tetraglyme and (b) 1.0 M-LiTFSI in EiPS.

Conclusions

We synthesized BQ derivatives bearing perfluoroalkyl groups and utilized them as positive-electrode materials for high-performance rechargeable batteries. CF_3-BQ exhibited a high first discharge capacity of 209 Ah/kg, which exceeds those of currently used LIBs. Previous rechargeable batteries using BQ derivatives as positive-electrode materials exhibited low discharge voltages. However, introducing electron-withdrawing groups in the BQ skeleton resulted in higher discharge voltages; e.g., CF_3-BQ exhibited a high average discharge voltage of 3.0 V versus Li/Li$^+$. Furthermore, batteries using CF_3-BQ, Rf_4-BQ, and Rf_6-Cl-BQ were stable against decomposition during charge-discharge processes in comparison to CH_3-BQ. This may be ascribed to the

stabilization of the radical and dilithium-salt states of these perfluoroalkylated BQs by Li-F interactions in the charge-discharge cycles; DFT calculations supported such stabilization. Electrolyte effects on the charge–discharge performance were also examined using CF_3-BQ, demonstrating the highest discharge capacity for the EiPS system, while the EC/DEC system provided the best cycle-life performance. Organic positive-electrode materials that accept two or more electrons afford higher energy densities and would be plausible alternatives to inorganic materials. However, the molecular design of these materials is difficult due to the paucity of information about the relationship between molecular structure and battery performance. We will continue to investigate this relationship to develop high-performance rechargeable batteries utilizing organic positive-electrode materials. Research into the viability of organic cathode active materials is in a very early stage. For example, battery components such as the electrolyte and separator (which considerably affect performance) have not been optimized for the such materials, although such studies have been initiated. Although the performance of organic positive-electrode materials, particularly with respect to cycle-life, is often inferior to inorganic materials at present, great improvements are anticipated as this research area matures.

Experimental

Cyclic voltammetry

CV was conducted in 1.0 mM solutions of samples in 0.1 M tetra-*n*-butylammonium perchlorate/acetonitrile (working electrode: glassy carbon; counter electrode: platinum wire; reference electrode: $Ag/AgNO_3$) system using a VSP multichannel Potentiostat/Galvanostat (Bio-logic). The voltammograms were recorded at a scan speed of 20 mV/s at room temperature. Potentials were corrected using the ferrocene/ferrocenyl couple (Fc/Fc^+) as an internal standard.

Preparation of coin cell and measurement of charge-discharge performance

For the coin-type cells, composites containing 3-5 wt% positive-electrode materials were fabricated with two compositions: 3:87:10 wt% positive-electrode materials, vapor-grown carbon fiber (VGCF), and poly(tetrafluoroethylene) (PTFE) (standard conditions); and 5:85:10 wt% positive-electrode materials, VGCF, and PTFE. A disc 12 mm in diameter was made by pressing the composite followed by drying *in vacuo*. A porous polymer film separator was sandwiched between the positive disc and a Li metal plate, and the resulting material was placed in a coin-type cell with the electrolyte solution. The electrolyte solutions were mixtures of EC and DEC (30:70 v/v) containing 1.0 M $LiPF_6$ (standard electrolyte solution); EiPS containing 1.0 M LiTFSI; and tetraglyme containing 4.8 M LiTFSI.

The charge-discharge measurements of the cells and cyclic voltammetry of the electrodes were performed using a KIKUSUI PFX2011 computer-controlled automatic battery charge and discharge instrument. The charge-discharge measurements of the cell were performed by the constant-current method at 0.1 mA in the cutoff voltage range of 1.5–4.2 V. Cyclic voltammetry of the electrodes was performed via three terminals connected to the coin-type cell, at a potential sweep rate of 0.33 mA/s and over a potential sweep range of 1.2–4.3 V.

DFT calculation

DFT calculations were carried out using the GAUSSIAN 09[16] program. Geometry optimizations were performed using standard gradient techniques at the B3LYP level of theory using restricted (RB3LYP) and unrestricted (UB3LYP) methods for closed- and open-shell systems, respectively.[17] In every case, 6-31+G* was used as the basis sets. All ground states were verified by vibration frequency analysis. The calculated molecular structures were visualized by Gauss View 4.1.

Notes and references

a Department of Chemistry, Graduate School of Science, Osaka Prefecture University, Sakai, Osaka, 599-8531, Japan. E-mail: matsu@c.s.osakafu-u.ac.jp

b Murata Manufacturing Co., Ltd., Nagaokakyo, Kyoto 617-8555, Japan. E-mail: m_satoh@murata.co.jp

† Electronic Supplementary Information (ESI) available: Table S1, Fig. S1, S2, and detailed information of DFT study. See DOI: 10.1039/b000000x/

1 (a) M. Armand and J.-M. Tarascon, *Nature*, 2008, **451**, 652-657; (b) B. Dunn, H. Kamath and J.-M. Tarascon, *Science*, 2011, **334**, 928-935; (c) Z. Yang, J. Zhang, M. C. W. Kintner-Meyer, X. Lu, D. Choi, J. P. Lemmon and J. Liu, *Chem. Rev.*, 2011, **111**, 3577-3613.

2 (a) J.-M. Tarascon and M. Armand, *Nature*, 2001, **414**, 359-367; (b) J. B. Goodenough and K.-S. Park, *J. Am. Chem. Soc.*, 2013, **135**, 1167-1176.

3 (a) V. Etacheri, R. Marom, R. Elazari, G. Salitra and D. Aurbach, *Energy Environ. Sci.*, 2011, **4**, 3243-3262; (b) K. Kanamura, *Lithium-Ion Batteries for Vehicles*, Nikkan Kogyo Shimbun LTD., Japan, 2010; (c) M. Watanabe, Advanced Batteries and Materials, Kyoritsu Shuppan Co., Ltd., Japan, 2012.

4   For a review of organic LIBs, see: Y. Liang, Z. Tao and J. Chen, *Adv. Energy Mater.*, 2012, **2**, 742-769.

5   For some recent work utilizing organosulfur compounds as positive-electrode material, see: (a) G. Weng, Y. Su, Z. Liu, Z. Wu, S. Chen, J. Zhang and C. Xu, *J. Appl. Polym. Sci.*, 2010, **116**, 727-735.; (b) Z. Shi-chao, Z. Lan, W. Wei-kun and X. Wen-juan, *Synth. Met.*, 2010, **160**, 2041-2044.; (c) P. Krishnan, S. G. Advani and A. K. Prasad, *J. Power Sources*, 2011, **196**, 7755-7759; (d) Y. Inatomi, N. Hojo, T. Yamamoto, S. Watanabe and Y. Misaki, *ChemPlusChem*, 2012, **77**, 973-976; (e) M. Kato, D. Ogi, M. Yao and Y. Misaki, *Chem. Lett.*, 2013, **42**, 1556-1558; (f) M. Kato, K. Senoo, M. Yao and Y. Misaki, *J. Mater. Chem. A*, 2014, **2**, 6747-6754; (g) T. Sarukawa and N. Oyama, *J. Electrochem. Soc.*, 2010, **157**, F23-F29; (h) T. Sarukawa, S. Yamaguchi and N. Oyama, *J. Electrochem. Soc.*, 2010, **157**, F196-F201; (i) R. A. Davoglio, S. R. Biaggio, R. C. Rocha-Filho and N. Bocchi, *J. Power Sources*, 2010, **195**, 2924-2927; (j) J. Fanous, M. Wegner, J. Grimminger, Ä. Andresen and M. R. Buchmeiser, *Chem. Mater.*, 2011, **23**, 5024-5028.

6   Some organosulfur compounds afforded high voltages, see references 5d-5h.

7   For some recent work utilizing organic radical compounds as positive-electrode material, see: K. Oyaizu, T. Sukegawa and H. Nishide, *Chem. Lett.*, 2011, **40**, 184-185.

8   For some recent work utilizing carbonyl compounds as positive-electrode material, see: (a) T. Nokami, T. Matsuo, Y. Inatomi, N. Hojo, T. Tsukagoshi, H. Yoshizawa, A. Shimizu, H. Kuramoto, K. Komae, H. Tsuyama and J. Yoshida, *J. Am. Chem. Soc.*, 2012, **134**, 19694-19700; (b) M. Yao, S. Yamazaki, H. Senoh, T. Sakai and T. Kiyobayashi, *Mater. Sci. Eng. B*, 2012, **177**, 483-487; (c) T. Sugimoto and K. Senoo, *Chem. Lett.*, 2012, **41**, 1475-1477; (d) H. Wu, K. Wang, Y. Meng, K. Lu and Z. Wei, *J. Mater. Chem. A*, 2013, **1**, 6366-6372; (e) Y. Liang and P. Zhang, J. Chen, *Chem. Sci.*, 2013, **4**, 1330-1337.

9   For some recent work of organic compounds not belonging to the three types for positive-electrode material, see: (a) J. K. Feng, Y. L. Cao, X. P. Ai and H. X. Yang, *J. Power Sources*, 2008, **177**, 199-204; (b) T. Matsunaga, T. Kubota, T. Sugimoto and M. Satoh, *Chem. Lett.*, 2011, **40**, 750-752; (c) M. Yao, H. Senoh, T. Sakai and T. Kiyobayasi, *J. Power Sources*, 2012, **202**, 364-368.

10   Some low-molecular-weight organic active materials afforded high cycle-life performance, see : (a) S. H. Lee, J.-K. Kim, G. Cheruvally, J.-W. Choi, J.-H. Ahn, G. S. Chauhan and C. E. Song, *J. Power Sources*, 2008, **184**, 503-507; (b) H. Chen, M. Armand, M. Courty, M. Jiang, C. P. Grey, F. Dolhem, J.-M. Tarascon and P. Poizot, *J. Am. Chem. Soc.*, 2009, **131**, 8984-8988; (c) M. Yao, M. Araki, H. Senoh, S. Yamazaki, T. Sakai and K. Yasuda, *Chem. Lett.*, 2010, **39**, 950-952; (d) S. Renault, J. Geng, F. Dolhem and P. Poizot, *Chem. Commun.*, 2011, **47**, 2414-2416; (e) Y. Morita, S. Nishida, T. Murata, M. Moriguchi, A. Ueda, M. Satoh, K. Arifuku, K. Sato and T. Takui, *Nat. Mater.*, 2011, **10**, 947-951; (f) W. Walker, S. Grugeon, H. Vezin, S. Laruelle, M. Armand, F. Wudl and J.-M. Tarascon, *J. Mater. Chem.*, 2011, **21**, 1615-1620.

11   For some work of polymerization reducing the capacity to much lower levels in benzoquinone derivatives, see: (a) J. S. Foos, S. M. Erker and L. M. Rembetsy, *J. Electrochem. Soc.*, 1986, **133**, 836-841; (b) T. L. Gall, K. H. Reiman, M. C. Grossel and J. R. Owen, *J. Power*

Sources, 2003, **119-121**, 316-320; (c) J. Xiang, C. Chang, M. Li, S. Wu, L. Yuan and J. Sun, *Cryst. Growth Des.*, 2008, **8**, 280-282.

12   (a) Y. Hanyu and I. Honma, *Sci. Rep.*, 2012, **2**, 453; (b) Y. Hanyu, Y. Ganbe and I. Honma, *J. Power Sources*, 2013, **221**, 186-190; (c) Y. Hanyu, T. Sugimoto, Y. Ganbe, A. Masuda and I. Honma, *J. Electrochem. Soc.*, 2014, **161**, A6-A9.

13   H. Senoh, M. Yao, H. Sakabe, K. Yasuda and Z. Siroma, *Electrochim. Acta*, 2011, **56**, 10145-10150.

14   (a) S. Tobishima, J. Yamaki and A. Yamaji, *J. Electrochem. Soc.*, 1984, **131**, 57-63; (b) M. Yao, H. Senoh, S. Yamazaki, Z. Siroma, T. Sakai and K. Yasuda, *J. Power Sources*, 2010, **195**, 8336-8340; (c) M. Yao, H. Senoh, M. Araki, T. Sakai and K. Yasuda, *ECS Trans.*, 2010, **28**, 3-10.

15   H. Matsubara, T. Maegawa, Y. Kita, T. Yokoji and A. Nomoto, *Org. Biomol. Chem.*, 2014, DOI: 10.1039/C4OB00783B.

16   Gaussian 09, Revision C.01, M. J. Frisch, G. W. Trucks, H. B. Schlegel, G. E. Scuseria, M. A. Robb, J. R. Cheeseman, G. Scalmani, V. Barone, B. Mennucci, G. A. Petersson, H. Nakatsuji, M. Caricato, X. Li, H. P. Hratchian, A. F. Izmaylov, J. Bloino, G. Zheng, J. L. Sonnenberg, M. Hada, M. Ehara, K. Toyota, R. Fukuda, J. Hasegawa, M. Ishida, T. Nakajima, Y. Honda, O. Kitao, H. Nakai, T. Vreven, J. A. Montgomery, Jr., J. E. Peralta, F. Ogliaro, M. Bearpark, J. J. Heyd, E. Brothers, K. N. Kudin, V. N. Staroverov, T. Keith, R. Kobayashi, J. Normand, K. Raghavachari, A. Rendell, J. C. Burant, S. S. Iyengar, J. Tomasi, M. Cossi, N. Rega, J. M. Millam, M. Klene, J. E. Knox, J. B. Cross, V. Bakken, C. Adamo, J. Jaramillo, R. Gomperts, R. E. Stratmann, O. Yazyev, A. J. Austin, R. Cammi, C. Pomelli, J. W. Ochterski, R. L. Martin, K. Morokuma, V. G. Zakrzewski, G. A. Voth, P. Salvador, J. J. Dannenberg, S. Dapprich, A. D. Daniels, O. Farkas, J. B. Foresman, J. V. Ortiz, J. Cioslowski, and D. J. Fox, Gaussian, Inc., Wallingford CT, 2010.

17   W. J. Hehre, L. Radom, P. v. R. Schleyer, P. A. Pople, *Ab Initio Molecular Orbital Theory*, Wiley, New York, **1986**.